



# Assessment of the performance of fibre optic sensor designs based on two FBGs

Jacek Palmowski<sup>1</sup> · Kamil Barczak<sup>2</sup> · Natalia Kubicka<sup>3</sup> · Franek Gołek<sup>4</sup> · Luke Benson<sup>5</sup> · Erwin Maciak<sup>2</sup> · Tadeusz Pustelny<sup>2</sup> · Sindy Phang<sup>6</sup> · Trevor Benson<sup>6</sup> · Elżbieta Bereś-Pawlik<sup>1,6</sup>

Received: 5 March 2024 / Accepted: 9 May 2024  
© The Author(s) 2024

## Abstract

The paper presents, and compares the performance of, two optical sensing systems each based on a combination of two fibre Bragg gratings (FBGs) and where a simple measurement of transmitted or reflected power provides an alternative to specialist interrogators. In both configurations one of the FBGs acts as a reference whilst the other is used as the measuring element. It is shown that using FBGs with wide spectra results in higher dynamic range. The measurement of strain is used to demonstrate the behaviour of the proposed sensing systems. The performance of the two systems is compared experimentally and discussed with the insight of the simultaneous measurement of the spectra reaching the detector.

**Keywords** Fiber Bragg gratings · Fibre optic sensing · Strain measurement · Environmental sensing

---

✉ Trevor Benson  
trevor.benson1@nottingham.ac.uk

<sup>1</sup> RELS Limited, Ul. Warciańska 18, 54-128 Wrocław, Poland

<sup>2</sup> The Faculty of Electrical Engineering, Silesian University of Technology, Ul. Krzywoustego 2, 44-100 Gliwice, Poland

<sup>3</sup> Faculty of Electronics and Information Technology, Warsaw University of Technology, Ul. Nowowiejska 15/19, 00-665 Warsaw, Poland

<sup>4</sup> Institute of Experimental Physics, University of Wrocław, Plac Maksa Borna 9, 50-204 Wrocław, Poland

<sup>5</sup> School of Physics and Astronomy, University of Leeds, Woodhouse Lane, Leeds LS2 9JT, UK

<sup>6</sup> George Green Institute for Electromagnetics Research, Faculty of Engineering, University of Nottingham, University Park, Nottingham NG7 2RD, UK

## 1 Introduction

The inscription of gratings in optical fibres to form a Fiber Bragg grating (FBG) creates a characteristic reflection spectrum. The shift of this spectrum when an FBG is subjected to an environmental parameter to be measured is the basis for various types of sensors (Grattan and Sun 2000). Fiber optic strain sensors based on FBGs have been reviewed by Campanella et al. (2018), with an emphasis on physical phenomena that can be sensed, the interrogation, and the read-out techniques. One measurement solution is to use an “interrogator” device or an optical spectrum analyser to directly measure the shift of this spectrum when a FBG is subjected to the environmental parameter to be measured. An alternate, lower-cost, approach is to convert the characteristic wavelength shifts of the FBG sensor into a power or voltage directly proportional to the measurement parameter. Davis and Kersey (1994) proposed and demonstrated an all-fibre configuration for this purpose. This was based on a wavelength-dependent  $2 \times 2$  fibre optic coupler, which exhibited a splitting ratio monotonically dependent on wavelength, and processing electronics. Further examples in the literature use two fibre Bragg gratings (FBGs) in various configurations, to provide suitable optical filtering and a measurement of the reflected or transmitted power that is proportional to the parameter to be measured, see for example (Ribeiro et al. 1997; Wade et al. 2010; Takahashi et al. 2001; Varghese et al. 2013; Pachava et al. 2015; Mądry et al. 2016). In these works, the FBG or laser measurement signal is characterised by a narrow spectral linewidth resulting in a measured power that is relatively small.

In this paper, we extend the work presented in Palmowski et al. (2023), which used measurement FBGs with wide spectral width, and compare two FBG sensor configurations, each based on two FBGs, in terms of their measurement capabilities and their sensitivity. In both systems one FBG is used as a reference and the other as the sensing element.

In the implementations reported in the present paper, the strain resulting from the elongation of the measurement fibre in a simple mechanical holder is determined. Such strain sensors can be used to measure the stress of the rock mass in mines, bridges, and transport (strain in aircraft wings, railway rails) etc. The sensing of strain and other environmental parameters, e.g., temperature and humidity, using FBGs has been widely reported (e.g., Wild and Richardson 2015; Qi et al. 2019; Shirayev et al. 2022; Mansoursamaei and Malakzadeh 2021; Bhaskar et al. 2021) and the two systems presented here can be readily adapted to these other sensing functions with the use of a suitable monitoring FBG.

The remainder of the paper is structured as follows. In Sect. 2 the measurement Systems A and B are described, along with the experimental arrangement used to evaluate them. The experimentally measured spectra of the narrow- and broadband FBGs used in the present work are presented. Experimental results on received power are presented in Sect. 3 and the sensitivity of each System is obtained. These results are discussed with the aid of measurements of the spectra entering the detector in Sect. 4. Finally, some Conclusions are drawn in Sect. 5.

## 2 Description of the measuring systems

The current paper presents and compares the measurement capabilities of two different measurement systems using two fibre Bragg gratings (FBGs). The two measurement systems are referred to as System A and System B. In both configurations one FBG is used for measurement and the other is used to provide a reference spectrum. Both

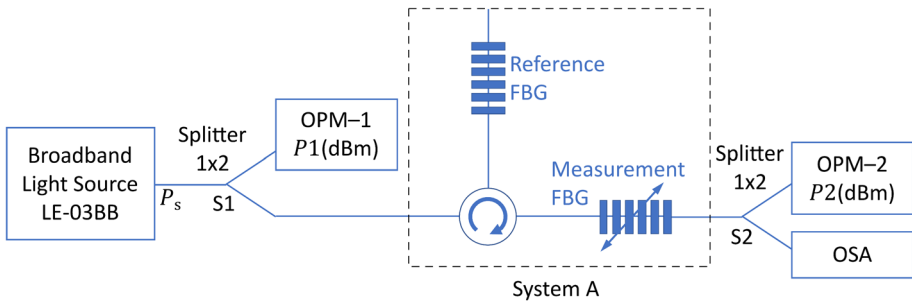


Fig. 1 Measurement System A placed within the experimental system used to evaluate its performance

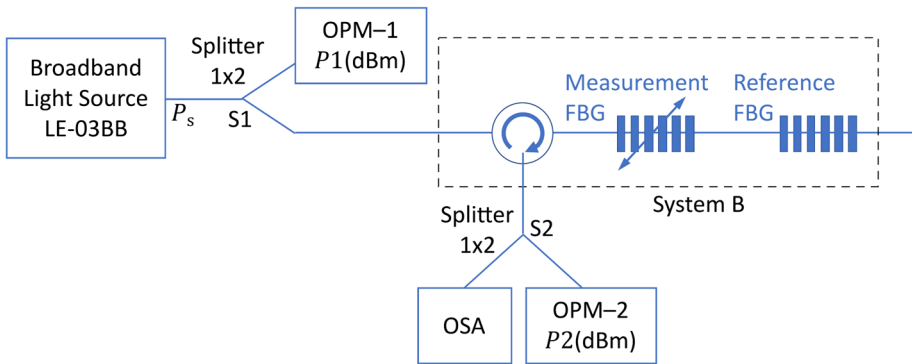
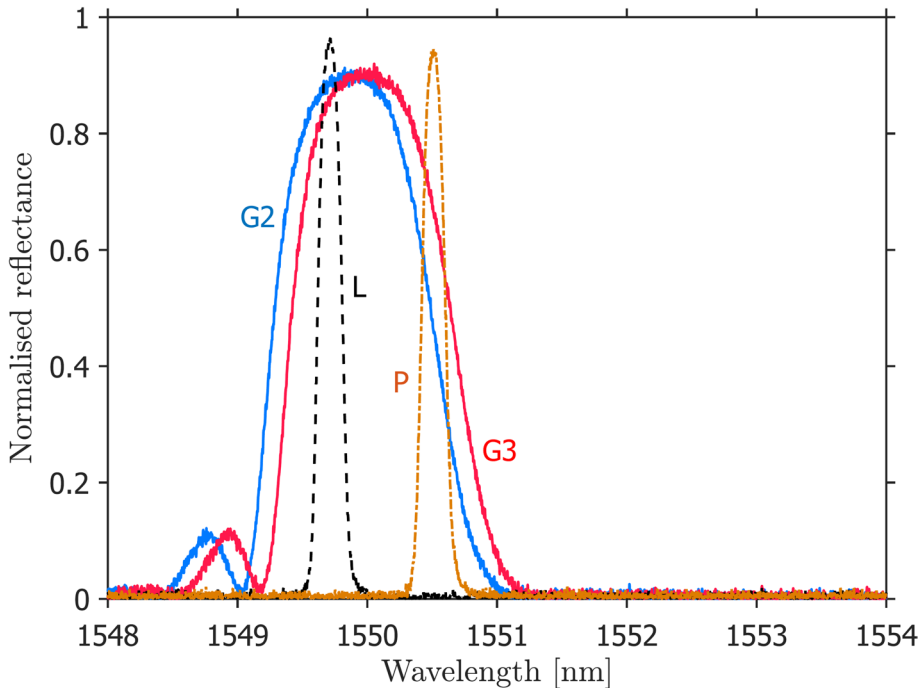


Fig. 2 Measurement System B placed within the experimental system used to evaluate its performance

systems allow changes in physical quantities (here illustrated by strain) to be determined by measuring changes in optical power. In measurement System A, shown in Fig. 1, the power of the light beam reflected from the reference FBG is modified by the measurement (transmission) FBG, which is subjected to strain or other environmental changes. System A was introduced by us in Palmowski et al. (2023) using a different pair of FBGs, where the detector used was a photodiode connected to a current to voltage converter targeting a low-cost sensor network able to store sensing information and/or communicate it to a base station. The idea of using a FBG to introduce a reference spectrum into a sensor FBG, as employed in System A, is similar to Takahashi et al. (2001). However, unlike in the present work, the reference spectrum produced in Takahashi et al. (2001) was a narrow-band one whose centre wavelength was matched to the slope of the reflection spectrum of the sensing FBG such that the intensity of the reflected light was modulated as the reflection spectrum of the sensor FBG varied. System B, shown in Fig. 2, measures the reflection from two FBGs arranged in series; once again, one of the FBGs is subject changes in the environmental parameter to be measured, here strain, and the other acts as a reference. The broadband light source used was a WT&T model LE-3BB (<https://www.wttechnology.com/>). Measurements were undertaken for a source power level ( $P_s$ ) of  $-14.05$  dBm; this corresponds to a power  $P_1$  of  $-17.6$  dBm measured on OPM-1. The sensing FBG was secured on a measurement rig described by us in Palmowski et al. (2023). It was stretched from its original length of  $\sim 10.0$  cm by

means of a mechanical micrometre, with the extension monitored using a dial gauge. The stretching introduces tensile strain into the test FBG, and this results in its reflection spectrum moving to higher wavelengths (see, for example, Palmowski et al. 2023). The introduction of the fibre splitters S1 and S2, each with a nominal splitting ratio of  $-3$  dB, enables simultaneous measurement of the powers shown as P1 and P2 using optical power meters (OPMs) and of the (output) spectrum entering the OPM-2 detector using a Yokohama AQ6374 optical spectral analyser (OSA). The manufacturer's data specifies that the  $-3$  dB splitter S1 divided power as  $-3.55$  dB and  $-3.61$  dB, and S2 as  $-3.67$  dB and  $-3.60$  dB. In each configuration the fibre components were coupled using standard single mode FC/APC connectors.

Figure 3 presents the reflection spectra of the two broadband FBGs (G2 and G3) and two narrowband FBGs (L and P) measured directly using the Yokohama AQ6374 optical spectral analyser at an input power  $P_s$  of  $-14.05$  dBm. Each reflectance presented is normalised to the manufacturer's cited maximum. All four FBGs were silica-based fibres manufactured by Safibra, <https://safibra.com/>.



**Fig. 3** The reflection spectra of the two broadband FBGs (G2 and G3) and two narrowband FBGs (L and P) used in the experiments reported. They were measured directly using the Yokohama AQ6374 optical spectral analyser at an input power  $P_s$  of  $-14.05$  dBm. Each plot is presented normalised to the manufacturer's cited maximum reflectivity (i.e. to 0.913 for G2, 0.920 for G3, 0.966 for L and 0.945 for P)

### 3 Experimental results for received power and determination of sensitivity

Figure 4 presents the change in the measured power  $P_2$  as a function of extension and indicative microstrain (i.e., extension divided by the original 10 cm length of the test FBG between the two fibre holders) for System A. The reference FBG is G2 and the test FBG in turn G3, L and P. Figure 5 presents the corresponding results for System B. It is clearly visible that in both Systems the use of a test FBG with a broadband spectrum gives bigger change in output power. Power meter readings had a precision of  $\pm 0.01$  dBm and the micrometre used to introduce the extension had a stated precision of 0.01 mm.

It is instructive to determine and compare the sensitivity of each System by plotting the Power  $P_2$  measured on OPM-2, converted to units of nW, as a function of extension and indicative microstrain. This is shown in Fig. 6 for test FBG G3. The figure indicates that both System A and System B exhibit a linear relationship between received power and extension over an extension range of around 0.25 mm (corresponding to a change in microstrain of  $2500 \mu\epsilon$ ). The linear fits shown for both Systems A and B on Fig. 6 have an  $R^2$  (square of correlation coefficient) value of 0.997 and 0.991 respectively. System A has a sensitivity (gradient) of  $0.035 \text{ nW}/\mu\epsilon$  and System B a sensitivity of  $0.047 \text{ nW}/\mu\epsilon$ . Figures 4 and 5 show that away from this region of change the received power in each System

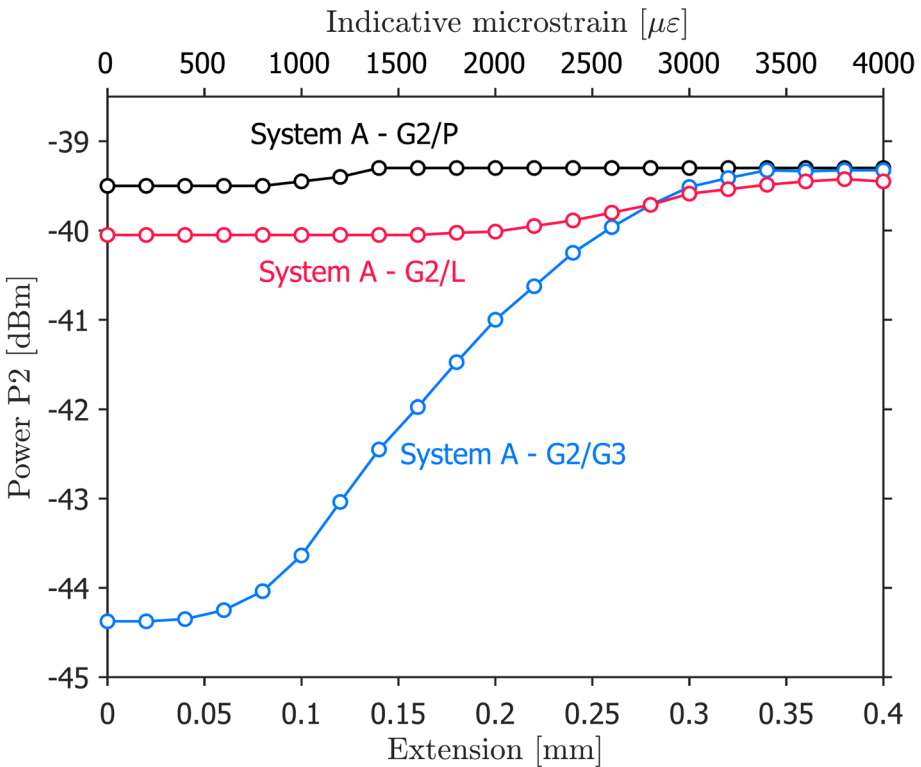
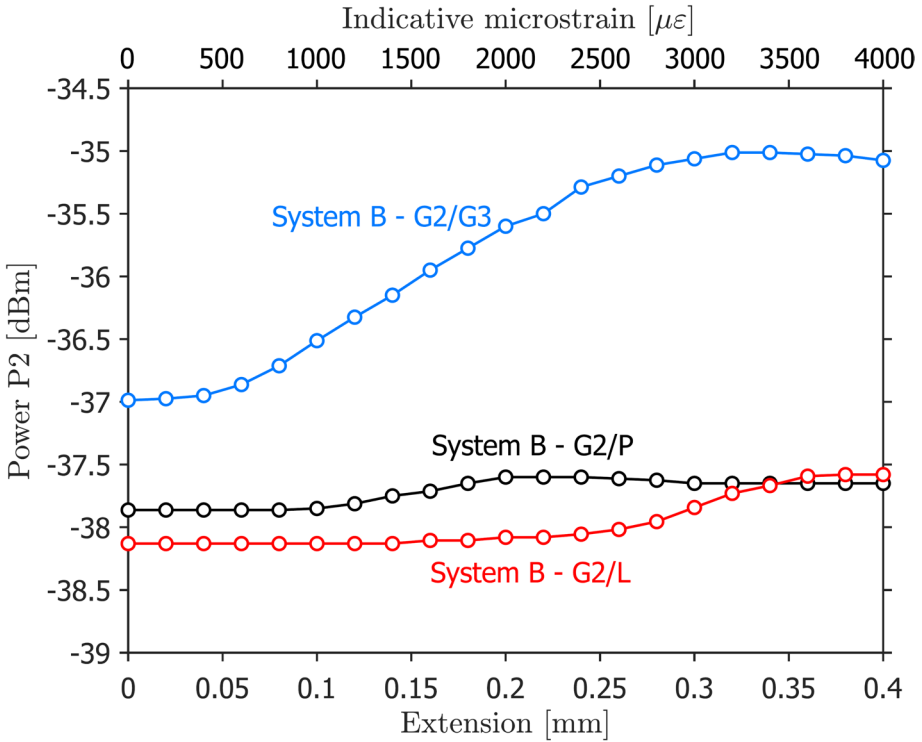


Fig. 4 Change in received optical power  $P_2$  during extension of test FBGs G3, L, P for System A. The Reference FBG was G2



**Fig. 5** Change in received optical power change P2 during extension of test FBGs G3, L, P for System B. The Reference FBG was G2

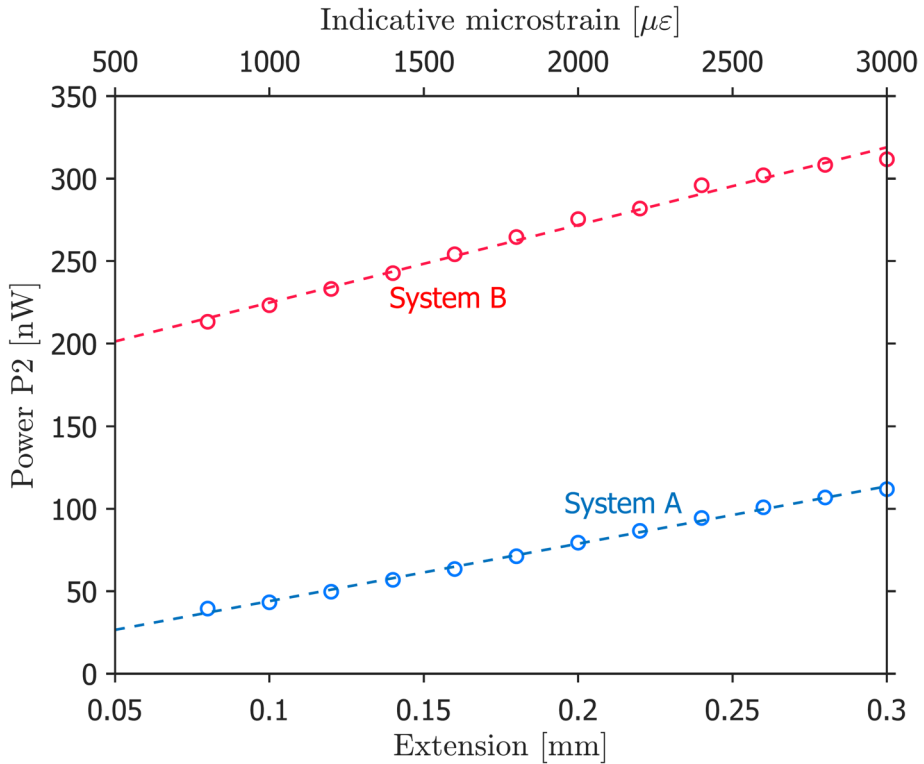
does not change much with the applied extension, facilitating their application in threshold detection.

Table 1 summarises some key results from the measurements presented in this section as an aid to further discussion.

#### 4 Discussion of power measurement results with the aid of measurements of spectra entering the detector

It is instructive to further compare and confirm the behaviour of the two Systems by studying the experimental spectral power densities at the detector (output) as a function of wavelength for various extensions. Figure 7 presents the power spectral densities for System A at various extensions for a reference FBG G2 and test FBGs L (top row), P (middle row) and G3 (bottom row.) These were obtained by normalising the spectral results obtained using the OSA such that the area under each curve gave the measured power. Corresponding results for System B are shown in Fig. 8.

Consider first the case when G3 is the test FBG. In System A the test FBG G3 is excited by the reference spectrum provided by FBG G2. As the test FBG G3 is extended, its reflection spectrum moves to longer wavelength; thus, its overlap with the spectrum of the reference FBG G2 reduces. Consequently, as shown in the bottom row in Fig. 7, FBG G3



**Fig. 6** Power  $P_2$  measured on OPM-2 and converted to units of nW plotted as functions of extension and indicative microstrain (i.e., extension divided by the original length of FBG G3). The gradients of the linear fits shown reveal that System A has a sensitivity (gradient) of 0.035 nW/ $\mu\epsilon$  (348 nW/mm for an unstretched length of 10.0 cm) and System B a sensitivity of 0.047 nW/ $\mu\epsilon$  (471 nW/mm for an unstretched length of 10.0 cm)

**Table 1** Summary of key results

FBG pair	Sensitivity, nW/mm		Dynamic range, dB		Approximate extension range over which a change in output is observed, mm	
	System A	System B	System A	System B	System A	System B
G2/G3	348	471	5.05	1.98	0.25	0.25
G2/L	74	93	0.60	0.55	0.20	0.22
G2/P	88	80	0.20	0.21	0.06	0.10

Dynamic range is the difference between maximum and minimum signals

reflects less of the reference spectrum and more power reaches the detector. Eventually the wavelength range over which FBG G3 reflects falls outside of the reference spectrum; thus, all the reference spectrum reaches the detector. This explains why a constant output power is received upon further extension. The test and reference FBGs are arranged in series in

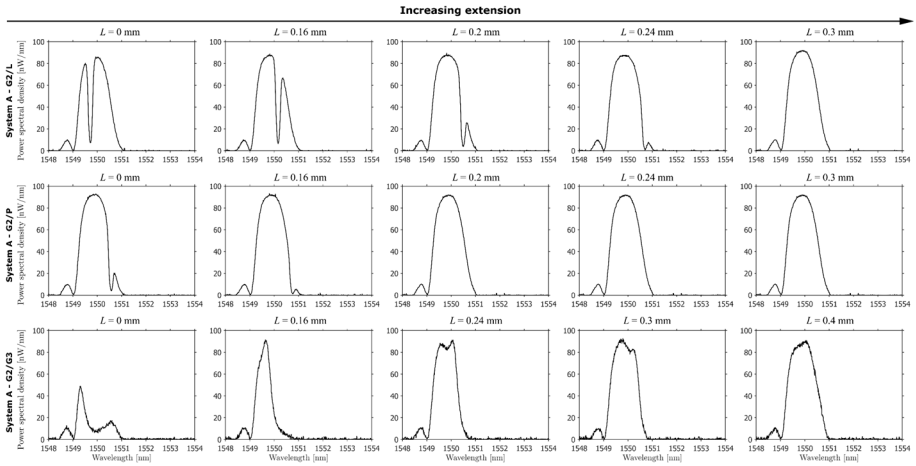


**Fig. 7** Output spectral power density as a function of wavelength for various extensions for System A. Top line G2/L, middle line G2/P, bottom line G2/G3. The curves were measured using the OSA shown in Fig. 1 and normalised such that the area under each curve gave the measured power P2

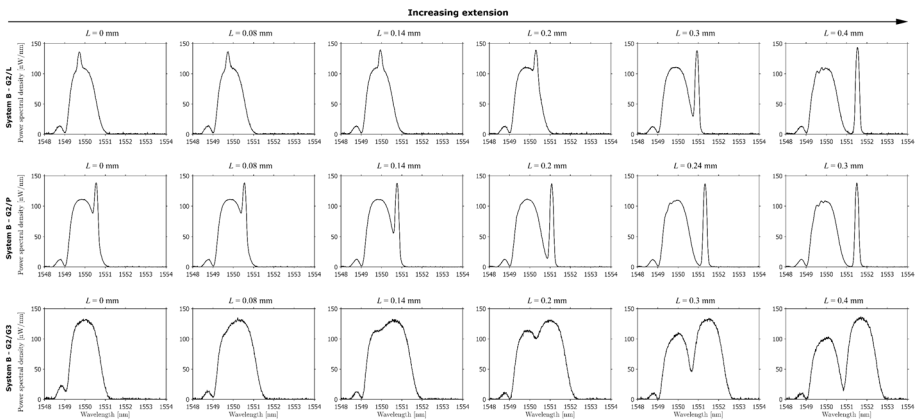


**Fig. 8** Output spectral power density as a function of wavelength for various extensions for System B. Top line G2/L, middle line G2/P, bottom line G2/G3. The curves were measured using the OSA shown in Fig. 2 and normalised such that the area under each curve gave the measured power P2

System B. The bottom line of Fig. 8 shows that as the test FBG G3 is extended, the spectra of the reflections from test and reference FBGs begin to separate. In the limit of large extension, it can be observed that the detector effectively receives the power reflected by each FBG. As the test and reference FBGs G2 and G3 have approximately the same bandwidth, the power received in Setup B at large extension is roughly double that received in Setup A—being the reflection from the reference G2 in System A (Fig. 7) and the reflection from G2 and the extended G3 in System B (Fig. 8). For intermediate extension multiple reflections are possible between the test and reference FBGs in System B.

The top and middle lines of Fig. 7 show that for the G2/L and G2/P combination of FBGs in System A the narrow bandwidth of FBGs test FBGs L and P prevent just a

small portion of the reference signal from reaching the detector. This explains why in Fig. 4 the received power for zero extension is much larger than that observed for the broadband test FBG G3 which at zero extension prevents a significant part of the reference spectrum from reaching the detector in this System. The central wavelength of FBG P lies close to the long wavelength edge of the reference spectrum; the spectrum of the test FBG P thus soon falls outside that of the reference on extension and all the reference signal then reaches the detector. FBG L behaves similarly but as the central wavelength of its reflection spectrum lies at a lower wavelength it blocks part of the reference signal from reaching the detector for a longer range of extensions.

The top and middle lines of Fig. 8 show that for the G2/L and G2/P combination of FBGs in System B the detected signal is an amalgamation of the power reflected from each FBG; as for the G2/G3 combination multiple reflections between the two FBGs are possible when their reflection spectra overlap. For large extensions the spectral range of the narrowband test FBGs falls outside that of the broadband reference and a sum of the reflections from each of the two reflections is observed. However, the narrower bandwidth of the FBGs L and P compared to that of FBG G3 means that a smaller amount of the source power reaches the detector. This explains why in Fig. 5 the output power for large extension is less than that observed for the combination G2/G3 of two broadband FBGs in System B.

## 5 Conclusions

The paper compares two optical sensing systems, each based on two FBGs where one of the FBGs acts as a reference and the other as the test FBG. In each System the power detected is related to the physical parameter to be measured, with changes in strain used in the paper for experimental demonstration purposes. Each System shows a larger dynamic range and higher sensitivity when using broadband FBGs as reference and test. In this case they each demonstrated a linear response over an extension range corresponding to 2500  $\mu\text{e}$ . Outside of this region of linear connection between output power and applied micro-strain, the output power does not vary much with applied strain in either System. This suggests a possible further application in threshold detection. Simultaneous measurement of the spectra of the signal reaching the detector using an OSA gives good insight into the behaviour of each sensing System. System B, with similar broadband FBGs used as reference and test, results in the largest detected power at large extension.

**Acknowledgements** TMB acknowledges, with thanks, the financial support of a Leverhulme Emeritus Fellowship, reference EM-2022-028.

**Authors' contributions** Experimental work was undertaken by J.P., K. B., N. K., F.G., L.B., E. M., T. P., T. B., and E. B-P. E. B-P., T. B., J.P, S.P., and L.B wrote the main manuscript text, undertook data analysis, and prepared figures. All authors reviewed the manuscript.

**Funding** Funding was provided by Leverhulme Trust (Grant No. EM-2022-028).

**Availability of data and materials** Contact Professor Dr Beres-Pawlik, elzbieta.berespawlik@gmail.com.

## Declarations

**Competing interests** None.

**Ethical approval** Not applicable. No human and/or animal studies.

**Open Access** This article is licensed under a Creative Commons Attribution 4.0 International License, which permits use, sharing, adaptation, distribution and reproduction in any medium or format, as long as you give appropriate credit to the original author(s) and the source, provide a link to the Creative Commons licence, and indicate if changes were made. The images or other third party material in this article are included in the article's Creative Commons licence, unless indicated otherwise in a credit line to the material. If material is not included in the article's Creative Commons licence and your intended use is not permitted by statutory regulation or exceeds the permitted use, you will need to obtain permission directly from the copyright holder. To view a copy of this licence, visit <http://creativecommons.org/licenses/by/4.0/>.

## References

- Bhaskar, C.V.N., Pal, S., Pattnaik, P.K.: Recent advancements in fiber Bragg gratings based temperature and strain measurement. *Results Opt.* **5**, 100130 (2021)
- Campanella, C.E., Cuccovillo, A., Campanella, C., Yurt, A., Passaro, V.M.N.: Fibre Bragg grating based strain sensors: review of technology and applications. *Sensors* **18**, 3115 (2018)
- Davis, M.A., Kersey, A.D.: All-fibre Bragg grating strain-sensor demodulation technique using a wavelength division coupler. *Electron. Lett.* **30**(1), 75–77 (1994)
- Grattan, K.T.V., Sun, T.: Fiber optic sensor technology: an overview. *Sens. Actuators* **82**(1–3), 40–61 (2000)
- Mądry, M., Markowski, K., Jędrzejewski, K., Bereś-Pawlik, E.: Power modulated temperature sensor with inscribed fibre Bragg gratings. *Opto-Electron. Rev.* **24**(4), 183–190 (2016)
- Mansoursamaei, M., Malakzadeh, A.: Simultaneous measurement of temperature and strain using a single fiber Bragg grating on a tilted cantilever beam. *Opt. Rev.* **28**, 289–294 (2021)
- Pachava, V.R., Kamineni, S., Madhuvarasu, S.S., Putha, K., Mamidi, V.R.: FBG based high sensitive pressure sensor and its low-cost interrogation system with enhanced resolution. *Photonic Sens.* **5**, 321–329 (2015)
- Palmowski, J., Barczak, K., Kubicka, N., Gofek, F., Benson, L., Maciak, E., Pustelny, T., Phang, S., Benson, T., Bereś-Pawlik, E.: Optical strain sensor with dual fibre Bragg grating topology. *Opt. Quant. Electron.* **55**(5), 453 (2023)
- Qi, Y., Jia, C., Tang, L., Wang, M., Liu, Z., Liu, Y.: Simultaneous measurement of temperature and humidity based on FBG-FP cavity. *Opt. Commun.* **452**, 25–30 (2019). <https://doi.org/10.1016/j.optcom.2019.07.0148>
- Ribeiro, A.L., Ferreira, L.A., Santos, J.L., Jackson, D.A.: Analysis of the reflective-matched fiber Bragg grating sensing interrogation scheme. *Appl. Opt.* **36**(4), 934–939 (1997)
- Shiryayev, O., Vahdati, N., Yap, F.F., Butt, H.: Compliant mechanism-based sensor for large strain measurements employing fiber optics. *Sensors* **22**, 3987 (2022). <https://doi.org/10.3390/s22113987>
- Takahashi, N., Yoshimura, K., Takahashi, S.: Fiber Bragg grating vibration sensor using incoherent light. *Jpn. J. Appl. Phys.* **40**, 3632–3636 (2001). <https://doi.org/10.1143/JJAP.40.363>
- Varghese, P.B., Kumar, R.D., Raju, M., Madhusoodanan, K.N.: Implementation of interrogation systems for fiber Bragg grating sensors. *Photonic Sens.* **3**, 283–288 (2013)
- Wade, S.A., Attard, D.P., Stoddart, P.R.: Analysis of transmission mode of a matched fiber Bragg grating interrogation scheme. *Appl. Opt.* **49**(24), 4498–4505 (2010)
- Wild, G., Richardson, S.: Analytical modeling of power detection-based interrogation methods for fiber Bragg grating for system optimization. *Opt. Eng.* **54**(9), 097109 (2015). <https://doi.org/10.1117/1.OE.54.9.097109>

**Publisher's Note** Springer Nature remains neutral with regard to jurisdictional claims in published maps and institutional affiliations.